Repeatable Acoustic Vaporization of Coated Perfluorocarbon Bubbles for Micro-Actuation Inspired by Polypodium aureum

Se-Yun Jeong , Han-Bok Seo , Myung-Hyun Seo , Jin-Woo Cho , Seho Kwon , Gihun Son , Seung-Yop Lee *

Posted Date: 8 January 2024

doi: 10.20944/preprints202401.0627.v1

Keywords: acoustic droplet vaporization; Polypodium aureum; perfluorocarbon; DDFP; contrast agent; micro actuator; microbot

Article

Repeatable Acoustic Vaporization of Coated Perfluorocarbon Bubbles for Micro-Actuation Inspired by *Polypodium aureum*

Se-Yun Jeong [1], Han-Bok Seo [1], Myung-Hyun Seo [1], Jin-Woo Cho [1], Seho Kwon [1], Gihun Son [1] and Seung-Yop Lee [1,2,*]

[1] Department of Mechanical Engineering, Sogang University, Baekbeom-ro 35, Mapo-gu, Seoul 04107, Republic of Korea
[2] Department of Biomedical Engineering, Sogang University, Baekbeom-ro 35, Mapo-gu, Seoul 04107, Republic of Korea
* Correspondence: sylee@sogang.ac.kr

Abstract: A fern, *Polypodium aureum*, possesses a specialized spore-releasing mechanism like a catapult induced by quick expansion of vaporized bubbles. This study introduces lipid-coated perfluorocarbon droplets to enable repeatable vaporization-condensation cycles, inspired by the repeatable vaporization of *Polypodium aureum*. Lipid-perfluorocarbon droplets have been considered not to exhibit repeatable oscillations due to bubble collapse by low surface tension of lipid layers. However, a single lipid-dodecafluoropentane droplet with a diameter of 9.17 μm shows expansion-contraction oscillations over 4,000 cycles by changing lipid composition and applying low power of 1.7 MHz ultrasound to induce partial vaporization of droplets. The optimal combinations of shell composition, droplet fabrication, and acoustic conditions can minimize damage on shell structure and quick recovery of damaged shell layers. The highly-expanding oscillatory microbubbles provide a new direction for fuel-free micro or nanobots as well as biomedical applications of contrast agents and drug delivery.

Keywords: acoustic droplet vaporization; Polypodium aureum; perfluorocarbon; DDFP; contrast agent; micro actuator; microbot

1. Introduction

In the past few decades, precise fabrication and actuation of micro or nano-sized objects have been actively developed to numerous fields such as biomedical imaging, therapy, and surgery [1-3] as well as nano or micro actuators and robots [4-6]. Various power sources such as chemical fuels, acoustic waves, magnetic fields, light, or thermal energy have been considered for the actuation of small-scale robots. However, new alternative fuels and propulsion mechanisms are necessary for safe and sustainable operation in the human body [4].

Numerous organisms in nature have efficiently functioning actuators across various sizes, serving as a great source of inspiration for technological advancements in human society. Various shooting mechanisms of spores and seeds in fungi and plants use water condensation, absorption and vaporization [7]. A representative example is a fern *Polypodium aureum*, belonging to the phelebodium genus (Figure 1(a)). *Polypodium aureum* possesses specialized sporangia for dispersing spores. The sporangium is composed of 12 to 13 annulus cells. As the annulus cells lose water by evaporation, water tension grows within them, thus causing the radial wall to shrink [8,9]. The force required to bend the annulus walls during opening is balanced by the negative pressure or water tension inside the cells. When the water tension is too large and the pressure falls below a critical threshold, cavitation bubbles are formed within several cells, leading to fast closure and ejection of the spores like a catapult [10], as illustrated in Figure 1(b). In this process, spores with a size of 300 μm are ejected at speeds of 10 m/s in just 10 μs [9]. The process of slow evaporation-quick vaporization could be repeated many times by placing the empty sporangium in water for a few

Preprints (www.preprints.org) | NOT PEER-REVIEWED | Posted: 8 January 2024 doi:10.20944/preprints202401.0627.v1

minutes [10]. It is worth noting that the specific structure and material of the annulus cells for spore release in *Polypodium aureum* provide the repetitive expansion-contraction motion without internal fuel or power. This study suggests the possible direction for the structural designs for self-powered micro actuators or long-lasting contrast agent, inspired by repeatable vaporization of *Polypodium aureum*.

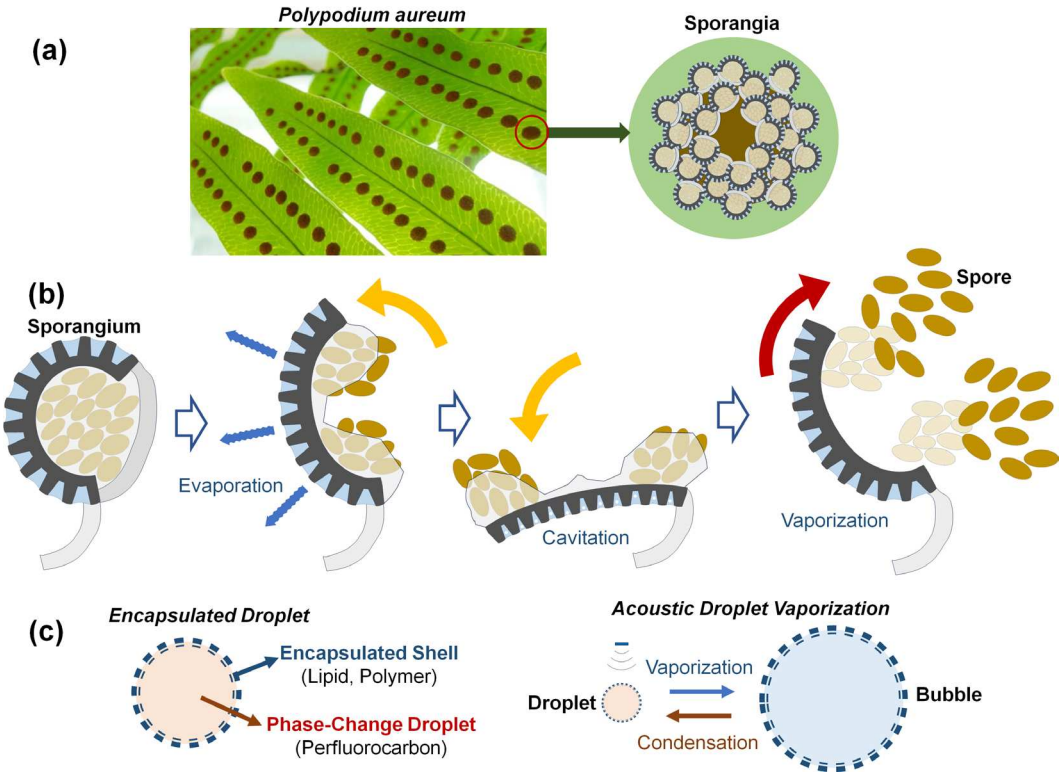

Figure 1. (a) Photo of a fern *Polypodium aureum* leaf containing the round, bright-orange clusters of sporangia. (b) Brief actuation mechanism of the sporangium to release spores based on the slow evaporation and quick cavitation vaporization. Sporangium opens as the annulus cells lose water by evaporation. Cavitation within the annular cells causes vaporization, leading to fast closure and ejection of spores in 10 ~ 30 ms [9,10]. (c) Encapsulated droplets of shell-perfluorocabon (PFC) exhibit size variation due to acoustic droplet vaporization (ADV) and bubble condensation at low temperatures.

Liquid droplets or gaseous bubbles undergo phase changes depending on the temperature, pressure, and medium conditions within a given system. As shown in Figure 1(c), external stimuli such as ultrasound, laser, and heat sources can cause size variation in droplets and bubbles due to vaporization or condensation [1-3]. The acoustic droplet vaporization (ADV) technique using phase-changing perfluorocarbon (PFC) droplets such as perfluoropentane (PFP), perfluorohexane (PFH), Perfluorobutane (PFB), and perfluorooctane (PFO), has shown great potential for diverse biomedical applications including local drug delivery to target tissues. There are two kinds of shell materials encapsulating phase change droplets. Hard shells use a coating of lower viscoelastic properties such as polymers or denatured proteins, as well as porous silica materials encapsulating gas. Generally, hard shell bubbles show an increased circulation time in vivo and are the preferred type of contrast agents for higher-intensity ultrasound applications [2]. Soft-shells using lipids or surfactant molecules are commonly used for examinations using a low mechanical index since these soft-shell bubbles are sensitively detectable due to the thinner, more flexible materials compared with hard-shell ones as well as the combination by hydrophobic interactions. Therefore, after slight shell disruptions, the shell seals itself to minimize surface tension [12]. If sealing is not possible due to the high acoustic pressure, the microbubbles will split into several smaller bubbles unlike the case of hard-shell microbubbles.

 doi:10.20944/preprints202401.0627.v1

PFC droplets vaporize at a negative pressure well above the ADV threshold. One or tens cycles of acoustically induced vaporization-condensation of lipid-PFC droplets have been reported in [13-15]. Marmottant et al. [15] observed expansion-contraction oscillations of a lipid-PFB droplet over 60 cycles when the acoustic pulse frequency increased from 1.5 to 4 MHz using low acoustic power to avoid shell buckling and bubble rupture.

The lipid-PFC droplets have been considered not to exhibit repeatable expansion-contraction oscillations due to the low mechanical properties of lipid layers. Encapsulated PFC droplets that demonstrate a large number of vaporization-condensation cycles by ADV have not yet been reported in literature. This study proposes a new fabrication method of lipid-PFC droplets to enable repeatable vaporization-condensation cycles over hundreds to thousands of times. The repeatable and stable oscillations are mainly induced by changing the shell-layer composition and applying lower ultrasound powers for partial vaporization of droplets to minimize damage on the shell structure and quick recovery of the damaged lipid layers.

2. Materials and Methods

2.1. Materials

Dodecafluoropentane (DDFP) from Synquest Labs (Alachua, FL, USA), was used as the core of PC droplets. DDFP has a boiling point of 29 °C at atmospheric pressure. The lipid shell encapsulating the PC droplet was fabricated using 1,2-ditearoyl-sn-glycero-3-phosphocholine (DSPC) and 1,2-dioctadecanoyl-sn-glycero-3-phosphoethanolamine - polyethylene glycol–2000 (DSPE-PEG2000), which were purchased from Avanti Polar Lipids (Alabaster, AL, USA). DSPC and DSPE-PEG2000 were dissolved in chloroform at molar ratios of 9:1 or 7:3 in a 2 mL clear vial. The vial was located in a vacuum chamber for 12 hours to completely remove the chloroform. Thereafter, a thin white lipid film that formed on the bottom of the vial was hydrated with 1.8 mL of distilled water and sonicated with a bath sonicator (Powersonic 505, Hwashin Intstrument, Seoul, Korea) at 56 °C. After the vial was rested with the lipid solution at room temperature, liquid DDFP was added to the vial to obtain a volume fraction of 10%. Finally, PC droplets were fabricated by agitating the vials for 45 sec in Vialmix (Lantheus Holdings, Billerica, MA, USA).

2.2. Experimetal Setup

The present experimental setup is shown in Figure 2. An acrylic water tank (0.3 m×0.2 m×0.1 m) filled with degassed water was placed on an inverted microscope (Epiphot 200, Nikon, Minato, TYO, Japan). A submersible heater was installed in the water tank to keep the water temperature at 24 or 36 °C. A high-intensity focused ultrasound (HIFU) transducer (PA 824, Precision Acoustics, Dorchester, Dort, UK) with a center frequency of 1.04 MHz was used to excite lipid cell-DDFP droplets. The amplitude of acoustic pressure and the excitation time were controlled by a function generator (33500B, Keysight, Santa Rosa, CA, USA). The signal from the function generator was amplified by 50 dB by the RF amplifier (A-075, Precision Acoustics) and transmitted to the active transducer. A manual trigger was used to provide five cycles of a sinusoidal wave in a total sonification time of 1 μs. For the repeatable vaporization and condensation experiments, a self-made ultrasound device was used to provide five ultrasonic frequencies (1, 1.7, 2.4, 3 and 5 MHz) with low powers, which is used to generate high-density nanobubbles [16].

A high-speed camera (VEO 410, Phantom, Wayne, NJ, USA) was integrated into the inverted microscope, allowing sample rates from 57,000 fps (17.54 μs) at a resolution of 256×256 pixels up to 250,000 fps (4 μs) at 128x64 pixels. The high-speed camera was synchronized with the function generator so that images were captured simultaneously with manual triggering. A 10× objective lens (PLN10X/0.25, Olympus, Shinjuku, TYO, Japan) and a 50× lens (CF Plan 50×0.55 EPI ELWD, Nikon) were used to magnify samples larger than 1 μm in diameter. The droplet samples were attached between two glass slides to observe their vaporization and condensation accurately. A microstage was used to place the active transducer where the highest ultrasonic pressure was measured. Once alignment was achieved, the inverted microscope and transducer were fixed on the optical table. The

Preprints (www.preprints.org) | NOT PEER-REVIEWED | Posted: 8 January 2024 doi:10.20944/preprints202401.0627.v1

droplet samples to be tested were optically and acoustically focused by moving a water tank using a linear stage installed on the microscope.

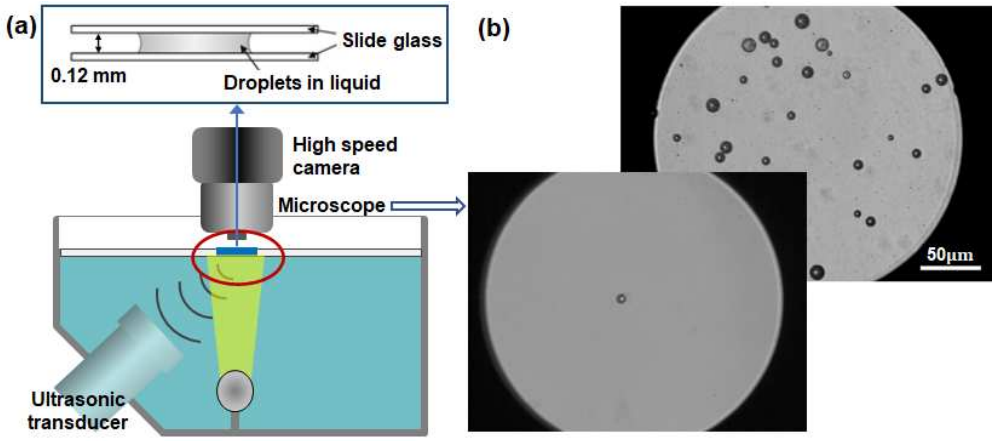

Figure 2. (a) Experimental setup composed of an ultrasonic transducer of 1.074MHz and a high-speed camera connected to an inverted microscope to capture lipid-DDFP droplets. (b) Microscopic images of micro-sized lipid-DDFP droplets.

3. Results and Discussion

3.1. Rescondensation after Vaporization and Bubble Collapse

The encapsulated droplets with diameters between 1.5 and 3.5 μm were tested to observe vaporization and recondensation. Figure 3(a) shows the timeline images of a single droplet with an initial diameter of 1.6 μm captured at every 4 μs when an ultrasound pulse of 1 μs at HIFU power of 10W was applied, and the water temperature was kept at 36 °C. The vaporized bubble kept expanding at 36 °C, which is above the boiling point (29 °C) of DDFP. The bubble diameter increased from 1.6 to 7.2 μm (approximately 2.8 times). However, when the temperature was set to be 24 °C below the boiling point (29 °C), the droplet with an initial diameter of 2.2 μm exhibited expansion by vaporization and then contraction by recondensation within 8 μs, as shown in Figure 3(b).

Figures 3(c) and 3(d) indicate the timeline of bubble diameter at 36 °C and 24 °C, respectively. Nine droplet samples with diameters between 1.5 and 3.5 μm were tested, and the average expansion ratio by acoustic vaporization was 3.68 (Figure 3(e)). The expansion ratio decreases slightly with increasing droplet size. The overshoot of transient shrinking and expanding motion observed after the first expansion at 8 μs indicates that the encapsulated shell composed of the lipid (DSPC) and the lipopolymer (DSPE-PEG2000) has elastic material properties. Similarly, different droplet samples with diameters between 1.5 and 3.5 μm were tested at 24 °C, and the bubble diameter variations before vaporization and after recondensation were measured. The average expansion ratio of the samples is 1.12 (Figure 3(f))

Preprints (www.preprints.org) | NOT PEER-REVIEWED | Posted: 8 January 2024 doi:10.20944/preprints202401.0627.v1

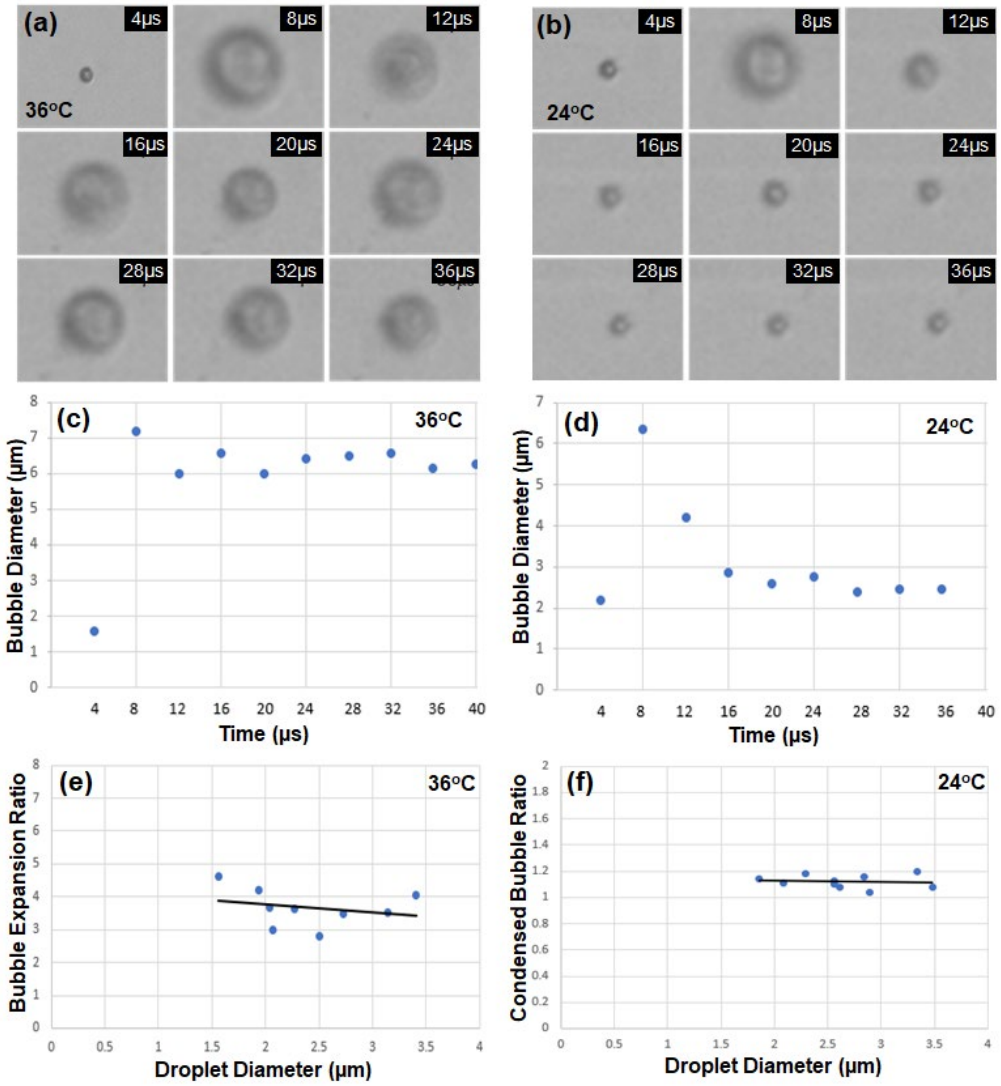

Figure 3. (a) The timeline images of a single droplet with an initial diameter of 1.6 μm, excited by an ultrasound pulse of 1 μs and power of 10 W at 36 °C. (b) The timeline images of a single droplet with an initial diameter of 2.2 μm at 24 °C. (c) The diameter of a droplet increased from 1.6 to 7.2 μm at 36 °C by an ultrasound pulse of 1 μs. (d) The droplet with an initial diameter of 2.2 μm exhibited vaporization and recondensation at 24 °C by an ultrasound pulse. (e) The bubble expansion ratios of nine droplet samples with diameters between 1.5 and 3.5 μm by acoustic vaporization at 36 °C. (d) The bubble diameter variations before vaporization and after recondensation of nine droplet samples at 24 °C.

In the previous experiments, droplet samples exposed to ultrasound power of 10 W disappeared due to shell collapse during vaporization. To compare the shell-collapse ratio by input power, the ultrasound power was increased to 20 W, and Figure 1(a) shows the collapsed motion of a single droplet sample at 24 °C. All encapsulated droplet samples disappeared at the power of 20 W. At high acoustic pressures, the droplet undergoes forced expansion and compression, which results in its destruction by either outward diffusion of the vaporized gas during the compression phase or diffusion via large shell defects, or by fragmentation [17]. Figure 4(b) compares the bubble collapse ratio at the power of 10 W and 20 W among the ten samples at 24 and 36 °C, respectively. The bubble survival rate without shell collapse at the power of 10 W is 50% and 30% for the cases of 24 and 36 °C, respectively. When 20 W pulses of ultrasound of 1.07 Hz were excited into the droplet samples at 24 °C, all the samples disappeared without repetitive vaporization and condensation cycles.

Preprints (www.preprints.org) | NOT PEER-REVIEWED | Posted: 8 January 2024 doi:10.20944/preprints202401.0627.v1

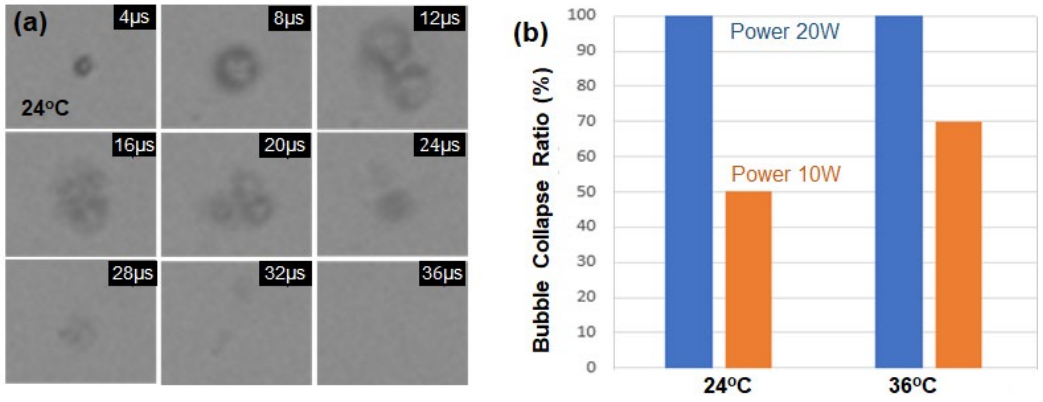

Figure 4. (a) The timeline images of a single droplet, excited by an ultrasound pulse of 1 μs and power of 20 W at 24 °C. (b) The bubble collapse ratio depending on the acoustic power (10 W and 20 W) and the temperature (24 and 36 °C).

3.2. Repetitive Vaporization-Condensation

One or tens cycles of acoustically induced vaporization-condensation of lipid-PFC droplets have been reported in [13-15]. The article [13] studied ADV dynamics containing three different formulations of PFC emulsions such as PFP, PFH, and PFO, observing that bubbles in PFO emulsions underwent repeated vaporization-recondensation or fragmentation. Namen et al. [14] demonstrated three consecutive vaporization-condensation cycles of nano-sized PFH droplets with lipid shells using 50 pulses of 10 cycles of HIFU and ultrasound B-mode image frames. The averaged peak diameter for the PFH samples was 558.71 ± 31.58 nm at an average concentration of 1.8x108 particles/mL. Marmottant et al. [15] observed expansion-contraction oscillations of a lipid-PFB droplet over 60 cycles in 35 μs when the acoustic pulse frequency increased from 1.5 to 4 MHz using low acoustic power to avoid shell buckling and bubble rupture. The oscillations of the bubble diameter, which were within 30% of the initial diameter, exhibited expansion-contraction cycles that decreased with increasing acoustic frequency and oscillation cycle.

Optically vaporization-condensation cycles have been reported using laser pulses [18]. In the report, indocyanine green (ICG) loaded PFP droplets having bovine serum albumin (BSA) shells were locally heated using laser input. Six vaporization-condensation cycles of 2.0 μm droplet were observed in response to six consecutive short-pulse laser excitation (5 ns duration, 800 nm wavelength) using a high-speed camera of 5,000,000 fps. It is noted that the droplet size remained unchanged after one hour post exposure of 6 consecutive laser excitations, indicating the stability of the 2.0 μm droplet. However, some larger droplets (> 7.5 μm) tended to grow continually into a large gas bubble after undergoing a single vaporization and contraction event. The bubble instability prevented repetitive optical droplet vaporization (ODV). Moreover, optical droplet vaporization of encapsulated PFC droplets via pulsed laser absorption limits the imaging depth and temporal resolution for the biomedical applications.

The repeatable vaporization-condensation of PFC droplets by acoustic excitations offers several benefits such as longer circulation times, extended imaging windows and higher sensitivity, as well as higher imaging depth and resolution [14, 19]. Encapsulated PFC droplets to demonstrate a large number of vaporization-condensation cycles by ADV have not yet been reported in literature. Several design parameters are involved in the mechanical properties and stability of the shell layers and the threshold of PFC droplets. Ultrasound frequency, power, pulse duration and focal distance to droplet samples are carefully controlled to minimize the collapse of vaporized bubbles. Compared to the previous experiments in section 3.1, the ratio of lipid (DSPC) and the lipopolymer (DSPE-PEG2000) was decreased from 9:1 to 8:2 or 7:3 to change the property and thinness of the shell layers. Secondly, disc-type ultrasonic transducers to change mega-hertz frequencies (1, 1.7, 2.4, 3 and 5 MHz) and power were manufactured, which were used to generate high-density nanobubbles [16].

Preprints (www.preprints.org) | NOT PEER-REVIEWED | Posted: 8 January 2024 doi:10.20944/preprints202401.0627.v1

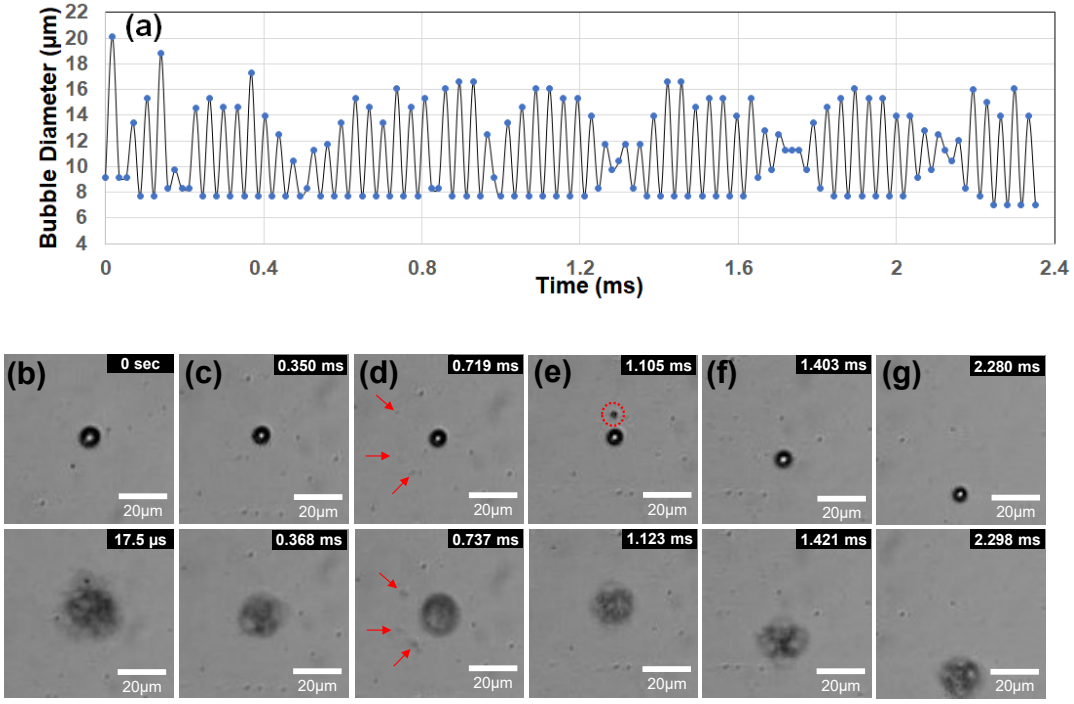

Figure 5. (a) A single lipid-DDFC droplet with an initial diameter of 9.17 μm exhibited 62 consecutive vaporization-condensation cycles using 1.7 MHz ultrasound and sampling time of 17.54 μs. (b)-(g) Six vaporization-condensation images of the droplet sample. After the first vaporization, the bubble size decreases slightly with increasing cycles. Bubble fragmentation was observed to occur due to the expanding and shrinking oscillations in (d) and (e).

Among various combinations of the design parameters, the conditions of 1.7 MHz ultrasound frequency, the low power of 3 W, and the 7:3 ratio of DSPC and DSPE-PEG2000 have generated stable vaporization and recondensation motions over 100 cycles. Figure 5(a) shows 62 consecutive vaporization-condensation cycles of a single lipid-coated DDFC droplet with an initial diameter of 9.17 μm using 1.7 MHz ultrasound. The bubble diameter of each image frame was measured using an open-source software ImageJ (www.imagj.net). The water temperature was kept at 24 °C. To observe the continuous movement of the excited droplet bubble, the frame rate of the high-speed camera was set to be 57,000 fps (17.54 μs) at a resolution of 256×256 pixels. The droplet sample showing the highest cycles could not be measured after 62 oscillation cycles (2.35 ms) because the bubble moved out of the focal image boundary rather than collapsing. The ultrasound frequency of 1.7 MHz imposes consecutive positive-negative pressure oscillations on the droplet with a period of 0.588 μs. The experimental results [15], which report 60 oscillation cycles of a lipid-PFB droplet in 35 μs using an ultra-speed camera of 15 Mfps (66.7 ns), clearly show that the droplet exhibited oscillatory motions responding to every oscillation of frequencies from 1.5 MHz to 4 MHz ultrasound. Therefore, the lipid-DDFP droplet in Figure 5(a) indicated vaporization-condensation oscillations of 4000 cycles (= 2.35 ms / 0.558 μs) by responding to every oscillation of 1.7 MHz ultrasound, and it represented the highest number of vaporization oscillations of lipid-PFC droplets published in literature to date.

The first vaporization image at 17.54 μs has the largest diameter of 20.14 μm over all the cycles, and the maximal expansion ratio is 2.2, which is lower than that in one cycle of vaporization-condensation in Figure 3(d). Therefore, it seems that the lower ultrasonic power leads to partial vaporization of the droplet, resulting in minimized damage on the shell structure, stable vaporization-condensation motions, and reduced oscillation period. The minimum diameters have changed little at the condensation stages since the bubble becomes more resistant to compression than to expansion [17], showing the non-linear oscillations due to high expansion and low contraction [15].

Preprints (www.preprints.org) | NOT PEER-REVIEWED | Posted: 8 January 2024 doi:10.20944/preprints202401.0627.v1

Figure 5(b)-(g) shows six different vaporization-condensation images of a single droplet. After the first vaporization, the bubble size decreases slightly with increasing cycles. When slight shell disruptions occur during expansion, the shell seals itself to minimize surface tension [12]. If sealing is not possible due to the high acoustic pressure, the expanding bubble will split into several smaller fragmentation bubbles instead of bursting like hard-shell encapsulated droplets [2]. As illustrated in Figure 5(d) and 5(e), bubble fragmentation was observed to occur due to the expanding and shrinking oscillations. It is also known that fragmentations become complete encapsulated droplets consisting of lipid shell and PFC core [17]. Lipid-coated fragmentations in Figure 5(d) are located away from the main droplet, and they expand individually without coalescence. On the contrary, a single fragmentation in Figure 5(e) merges into the main bubble during the subsequent vaporization. Small split fragmentations were observed in 9.6% of the 135 image frames captured with a time interval of 17.54 μs. Most of the fragmentations underwent coalescence during the additional vaporizations of the main droplet.

3.3. Future Direction for Micro-Sized Actuation and Biomedical Applications

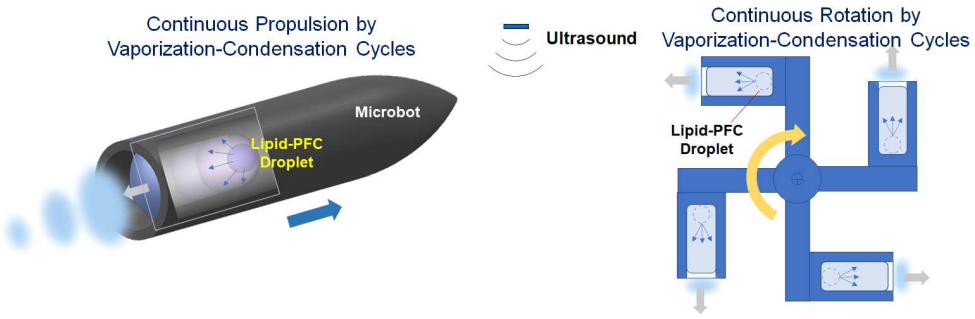

Figure 6. Concepts of linear and rotational micro-actuators using repeatable vaporization-condensation cycles of lipid-coated PFC bubbles.

Various types of microbots or nanobots based on distinct actuation principles using chemical fuels, acoustic waves, magnetic fields, light, or thermal energy have been developed in the past decade [4-6]. Ultrasound can realize noninvasive and on-demand motion control with long lifetime and good biocompatibility when it is used as external energy input to micro actuators [6]. Moreover, acoustic actuation offers many advantages in terms of strong penetration, high flexibility, and good biocompatibility, making it highly desirable for many emerging fields [20]. Figure 6 shows two typical fields of micro actuators based on linear and rotational propulsions. Many types of acoustically driven actuators have been developed such as acoustically propelled rod/wire/tube microbots, acoustically resonated microbubble actuators, acoustic motors/pumps, and acoustic tweezers [20-23]. Acoustic bubble actuators use the resonance behavior of trapped air bubbles, as the acoustic frequency approaches the resonance frequency of the bubbles [5]. However, the propulsion power is relatively small due to the low expansion ratio at resonance.

Micro actuators using phase-change droplets have been applied to short-time expansion and propulsion, such as contrast agents [2,3], microbullets [24], and microcannons [25]. Thin lipid layers with low surface tension, as shell materials, are considered inadequate for use in repeatable expansion-contraction oscillations of phase-change bubbles. This study proposes a new direction for the biomedical applications of highly-expanding oscillatory bubbles by demonstrating thousands of vaporization-condensation oscillations of lipid-DDFP droplets. However, there are still many problems to be solved for the use of long-time oscillating bubbles.

To improve the robust oscillations of lipid-coated PFC droplets, optimal combinations of design parameters such as shell composition and mixture ratio, droplet fabrication technique, acoustic frequency and power, and experimental setups are important. A variety of techniques have been developed for the fabrication of PFC droplets such as agitation, sonication, extrusion, condensation, and microfluidic techniques [3]. In particular, shell materials and composition ratios that provide

higher surface tension, lower gas leaking, and faster damage recovery should be developed to enhance the stability and durability of the coated droplets. These materials could include various lipids (DSPC, DMPC, DBPC) and lipopolymers (PEG40S, DSPE-PEG350/750/2000) [26,27] and new shell compounds of PEG-based polymers, including diblock copolymer constructs [4].

4. Conclusions

This study introduced lipid-coated DDFP droplets to enable repeatable vaporization-condensation cycles, inspired by the repeatable vaporization of *Polypodium aureum*. A single encapsulated DDFP droplet with a diameter of 9.17 μm exhibited expansion-contraction oscillations over 4,000 cycles, which is the highest number of vaporization oscillations published in literature to date. The highly repeatable microbubble was fabricated by using the lipid composition of the 7:3 ratio between DSPC and DSPE-PEG200, and it was excited by low power (5 W) of 1.7 MHz ultrasound to cause partial vaporization of droplets and minimize damage on shell structure. The highly-expanding oscillatory microbubbles provide a new direction for fuel-free micro or nanobots as well as biomedical applications of contrast agents and drug delivery.

Author Contributions: Conceptualization, S.Y.J., H.B.S. and S.Y.L.; methodology, S.Y.J. and M.H.S.; software, J.W.C.; validation, J.W.C., S.K. G.S. and S.Y.L.; formal analysis, G.S. and S.Y.L.; investigation, S.Y.J., M.H.S. and H.B.S.; writing—original draft preparation, S.Y.J. and S.Y.L.; writing—review and editing S.Y.L.; supervision, G.S. and S.Y.L.; funding acquisition, S.Y.L. All authors have read and agreed to the published version of the manuscript.

Funding: This research was funded by the National Research Foundation of Korea, grant number 2021R1A2C2012333.

Institutional Review Board Statement: Not applicable

Data Availability Statement: The data that support the findings of this study are available from the corresponding author upon reasonable request.

Conflicts of Interest: The authors declare no conflict of interest.

References

1. Upadhyay, A.; Dalvi, S.V. Microbubble Formulations: Synthesis, Stability, Modeling and Biomedical Applications. *Front. Pharmacol.* **2019,** *45*, 301-343.
2. Paefgen, V.; Doleschel, D; Kiessling, F. Evolution of Contrast Agents for Ultrasound Imaging and Ultrasound-Mediated Drug Delivery. *Ultrasound Med. Biol.* **2015,** *6*, 197.
3. Lea-Banks, H.; O'Reilly, M.A.; Hynynen, K. Ultrasound-Responsive Droplets for Therapy: A Review. *J. Control. Release.* **2019** *293*, 144-154.
4. Li, J. de Ávila, B.E.-F.; Gao, W.; Zhang, L.; Wang. J. Micro/Nanorobots for Biomedicine: Delivery, Surgery, Sensing, and Detoxification. *Sci Robot* **2017**, *2*, eaam6431
5. Chen, X.Z.; Jang, B.; Ahmed, D.; Hu, C.; De Marco, C.; Hoop, M.; Mushtaq, F.; Nelson, B.J.; Pané, S. Small-Scale Machines Driven by External Power Sources. *Adv. Mater*. **2018,** *30*, e1705061.
6. Wang, B.; Kostarelos, K.; Nelson, B.J.; Zhang, L. Trends in Micro-/Nanorobotics: Materials Development, Actuation, Localization, and System Integration for Biomedical Applications. *Adv. Mater*. **2021,** *33*, 202002047.
7. Sakes A.; van der Wiel, M.; Henselmans, P.W.J.; van Leeuwen, J.L.; Dodou, D.; Breedveld, P. Shooting Mechanisms in Nature: A Systematic Review. *PLOS One*, **2016**, *11*, e0158277.
8. Noblin, X.; Rojas, N.O.; Westbrook, J.; Llorens, C.; Argentina, M.; Dumais, J. The Fern Sporangium: A Unique Catapult. *Science* **2012**, *335*, 1322.1322.
9. King, A.L. The Spore Discharge Mechanism of Common Ferns. *Proc. Natl Acad. Sci.* **1944**, *30*, 155–161.
10. Llorens, C.; Argentina, M.; Rojas, N.; Westbrook, J.; Dumais, J.; Noblin, X. The Fern Sporangium: A Unique Catapult, The Fern Cavitation Catapult: Mechanism and Design Principles. *Interface* **2016**, *13*, 25150930.
11. Aliabouzar, M.; Kripfgans, O.D.; Fowlkes, J.B. Fabiilli. Bubble Nucleation and Dynamics in Acoustic Droplet Vaporization: A Review of Concepts, Applications, and New Directions. *Z. Med. Phys.* **2023**, *33*, 387–406.
12. Borden, M.A.; Kruse, D.E.; Caskey, C.F.; Zhao, S.; Dayton, P.A.; Ferrara, K.W. Influence of Lipid Shell Physicochemical Properties on Ultrasound- Induced Microbubble Destruction. *IEEE Trans. Ultrason. Ferroelectr. Freq. Control* **2005**, *52*, 1992-2002.

13. Aliabouzar, M.; Kripfgans, O.D.; Estrada, J.B.; Fowlkes, J.B. Fabiilli, M.L. Multi-Time Scale Characterization of Acoustic Droplet Vaporization and Payload Release of Phase-Shift Emulsions using High-Speed Microscopy. *Ultrason. Sonochem.* **2022**, *88*. 106090.
14. Namen, A.V.; Jandhyala, S.; Jordan, T.; Luke, G.P. Repeated Acoustic Vaporization of Perfluorohexane Nanodroplets for Contrast-Enhanced Ultrasound Imaging. *IEEE Trans. Ultrason. Ferroelectr. Freq. Control* **2021**, *68*, 3497-3506.
15. Marmottant, P.; van der Meer, S.; Emmer, M.; Versluis, M.; de Jong, N.; Hilgenfeldt, S.; Lohse, D. A Model for Large Amplitude Oscillations of Coated Bubbles Accounting for Buckling and Rupture, *J. Acoust. Soc. Am*. **2005**, *118*, 3499–3505.
16. Seo, H.-B.; Lee, S.-Y. High-Concentration Nanobubble Generation by Megasonic Cavitation and Atomization. *Coll. Interf. Sci. Commun*. **2023**, *52*, 100687.
17. Hernot, S.; Klibanov, A.L. Microbubbles in Ultrasound-Triggered Drug and Gene Delivery. *Adv. Drug Deliv. Rev.* **2008**, *60*, 1153–1166.
18. Yu, J.; Chen, X.; Villanueva, F.S.; Kim, K. Vaporization and Recondensation Dynamics of Indocyanine Green-Loaded Perfluoropentane Droplets Irradiated by a Short Pulse Laser. *Appl. Phys. Lett*. **2016**, *109*, 243701.
19. Fabiilli, M.L.; Haworth, K.J.; Fakhri, N.H.; Kripfgans, O.D.; Carson, P.L.; Fowlkes, J.B. The Role of Inertial Cavitation in Acoustic Droplet Vaporization. *IEEE Trans. Ultrason. Ferroelectr. Freq. Control* **2009**, *56*, 1006-3497-3506.
20. Xiao, Y.; Zhang, J.; Fang, B.; Zhao, X.; Hao, N. Acoustics-Actuated Microrobots. *Micromachines* **2022**, *13*, 481.
21. Li, J.; Mayorga-Martinez, C.C.; Ohl, C.-D.; Pumera, M. Ultrasonically Propelled Micro- and Nanorobots. *Adv. Funct. Mater* **2022,** *32*, 2102265.
22. Gao, Y.; Wu, M.; Lin, Y.; Zhao,W.; Xu, J. Acoustic bubble-based bidirectional micropump. *Microfluid. Nanofluidics* **2020**, *24*, 29.
23. Jang, D.; Jeon, J.; Chung, S.K. Acoustic Bubble-Powered Miniature Rotor for Wireless Energy Harvesting in a Liquid Medium, *Sens. Actuator A Phys.* **2018**. *276*, 296-303.
24. Kagan, D.; Benchimol, M.J.; Claussen, J.C.; Chuluun-Erdene, E.; Esener, S.; Wang, J. Acoustic Droplet Vaporization and Propulsion of Perfluorocarbon-Loaded Microbullets for Targeted Tissue Penetration and Deformation, *Angew. Chem*. **2012**, *124*, 7637-7640.
25. Soto, F.; Martin, A.; Ibsen, S.; Vaidyanathan, M.; Garcia-Gradilla, V.; Levin, Y.; Escarpa, A.; Esener, S.C.; Wang, J. Acoustic Microcannons: Toward Advanced Microballistics. *ACS Nano* **2016**, *10*, 1522.
26. Kowalska, M.; Broniatowski, M.; Mach,M.; Płachta, Ł.; Wydro, P. The Effect of the Polyethylene Glycol Chain Length of a Lipopolymer (DSPE-PEGn) on the Properties of DPPC Monolayers and Bilayers. *J. Mol. Liq*. **2021**, 335, 116529.
27. Kwan, J.J.; Borden M.A. Lipid Monolayer Collapse and Microbubble Stability. *Adv. Coll. Int. Sci*. **2012**, *183*, 82-99